Fully Integrated Indium Gallium Zinc Oxide NO2 Gas Detector

Fully Integrated Indium Gallium Zinc Oxide NO_2 Gas Detector

Mani Teja Vijjapu[1‡], Sandeep G. Surya[1‡], Saravanan Yuvaraja[1], Xixiang Zhang[2], Husam N. Alshareef[2], and Khaled N. Salama[*1]

[1]Sensors lab, Advanced Membranes and Porous Materials Center, Computer, Electrical and Mathematical Science and Engineering Division, King Abdullah University of Science and Technology (KAUST), Thuwal, 23955-6900, Kingdom of Saudi Arabia

[2]Physical Sciences and Engineering Division, King Abdullah University of Science and Technology (KAUST), Thuwal, 23955-6900, Kingdom of Saudi Arabia

KEYWORDS: Gas sensor, thin film transistor, IGZO TFT, integrated gas detector, room temperature, metal oxide sensor

ABSTRACT: We report an amorphous indium gallium zinc oxide (IGZO) based toxic gas detection system. The microsystem contains an IGZO thin film transistor (TFT) as a sensing element and exhibits remarkable selectivity and sensitivity to low concentrations of nitrogen dioxide (NO_2). In contrast to existing metal oxide based gas sensors, which are active either at high temperature or with light activation, the developed IGZO TFT sensor is operable at room temperature and requires only visible light activation to revive the sensor after exposure to NO_2. Furthermore, we demonstrate air-stable sensors with an experimental limit of detection of 100 ppb. This is the first report on metal oxide TFT gas sensors without heating or continuous light activation. Unlike most existing gas sensing systems that take care of identifying the analytes alone, the developed IGZO microsystem not only quantifies NO_2 gas concentration but also yields 5-bit digital output. The compact microsystem incorporating readout and analog to digital conversion modules developed using only two TFTs, paves the way for inexpensive toxic gas monitoring systems.

Air quality has a profound influence on human health, but rapid industrialization and urbanization have resulted in pollution worldwide due to automobile and industry emissions outgassing various toxic gases.[1] Automobile emissions are one of the major sources of pollution, among which nitrogen oxides (NO_x) are major constituents of concern as they lead to particulate matter ($PM_{2.5}$) production.[2] Hence, there is a burgeoning demand for cost-effective air quality monitoring stations using low-cost gas sensors.[3-4] The need for an accurate and economical way of sensing toxic gases has triggered interest in exploring inexpensive, highly sensitive, selective gas sensors.[5-9] Among all these gases, as per Occupational Safety and Health Administration (OSHA) limits, NO_2 has a meager short time exposure limit (STEL) as 1 ppm, which means the exposure limit of 1 ppm NO_2 is 15 minutes. Changes in pulmonary functions in healthy patients are evident for 2-3 ppm exposure of NO_2.[10] 4 hours of lethal concentration (LC_{50}) NO_2 is estimated to be 90ppm,[10] and exceeding this limit has adverse effects on human respiratory systems, such as causing asthma[11] and chronic pulmonary diseases.[12] Hence, detection of NO_2 with higher sensitivity, selectivity, and the lower detection limit is vital for human health and safety.

Conventional gas sensing technologies that are being researched are electrochemical,[13] semiconducting metal oxide based (SMO),[14-15] optical,[16] acoustic,[17] chromatography[18], and calorimetric[19] technologies. In particular, SMO gas sensors are shown to fulfill most of the criteria for gas sensing applications.[20] Many efforts are being made to enhance the sensitivity and selectivity of these sensors by exploring metal oxide nanoparticles,[21] nanocomposites,[22] nanostructures[23], and metal-organic frameworks,[24-26] thereby increasing the surface to volume ratio and the number of reactive sites to enhance gas diffusion. Although many gas and vapor sensors based on nanomaterials have been reported, implementing them in the system for real-time applications is a great challenge because of mass production and reproducibility issues. Complementary MOS (CMOS) compatible sensors that can be easily integrated with CMOS circuitry have considerable potential in realizing gas sensing systems.[27] However, existing SMO gas sensors are power-hungry since they are active either at high temperatures (>200 ^oC)[20] or with light activation. Furthermore, high-temperature SMO sensors cannot be used in some critical environments, such as if there is a chance of flammable or explosive gas leak whose ignition temperatures are in the range of the operating temperatures of these sensors; namely, H_2S has ignition point of 260 ^oC.[28] Light-activated SMO devices are the apparent choice in such cases, but sensitivity is very low when compared to thermally activated devices because of the limited optical response.[29] Recently, for low concentration NO_2 detection, a zinc oxide nanoparticle-based light active electrochemical sensor has been reported, but it must be turned on all the time to keep the sensing layer active,[21] making it power-hungry. Hence, developing an SMO sensor that is active at room temperature and without continuous light activation is crucial.

Nomura et al.[30] reported a thin film transistor (TFT) utilizing indium gallium zinc oxide (IGZO) for the first time. It had promising properties, such as high carrier mobility and high carrier concentration, making it the best semiconducting channel candidate for the TFTs.[31] However, non-passivated IGZO TFT's electrical characteristics are sensitive to ambient oxygen.[32] There are some reports on IGZO as an active layer to detect NO_2,[33-36] but these sensors require either UV activation[35] or high temperature for sensing and recovery,[33-34, 36] which are typical requirements of SMO gas sensors. In the present work, we propose a gas sensor using IGZO as the active layer for sensing NO_2 at room temperature without continuous light activation. The way to recover these devices after exposure is through light illumination, which is a more power-efficient solution than existing SMO gas sensors since it does not require high temperature or continuous light activation for sensing.

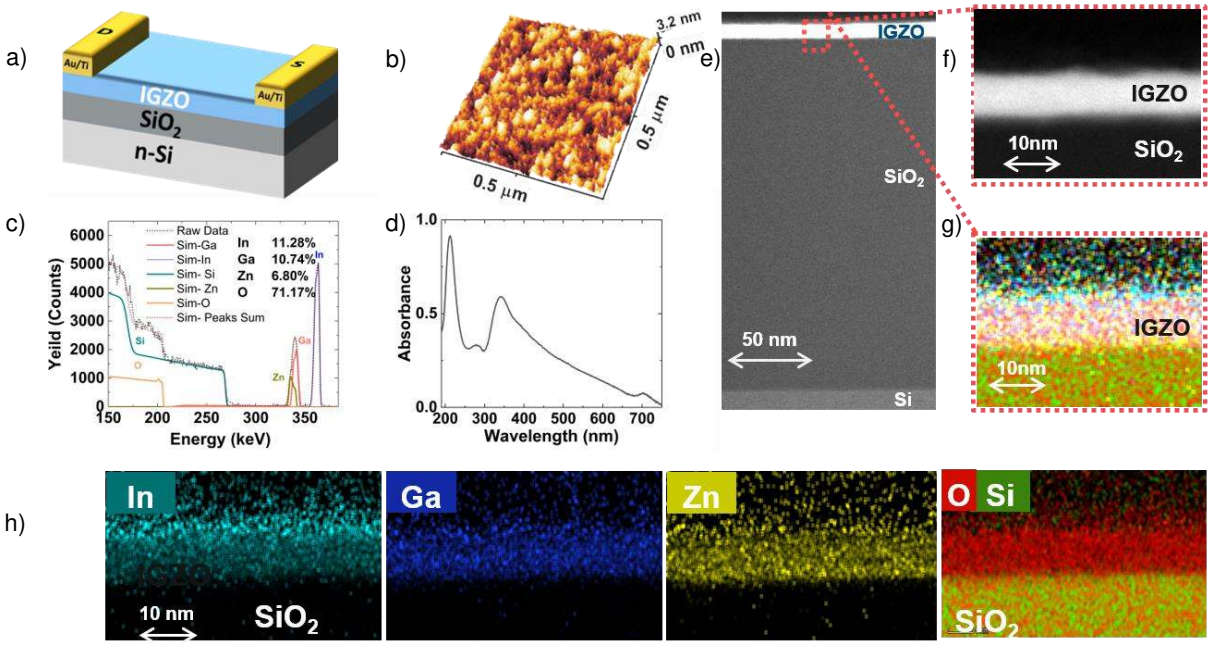

Figure 1a) Schematic of the fabricated Indium Gallium Zinc Oxide (IGZO) thin film transistor (cross-section) with IGZO as channel and active sensing layer with the Ti/Au as Source and Drain electrodes of the transistor. b) Atomic Force Microscopy (AFM) image of the IGZO with the mean roughness of 0.23 nm. c) High-resolution Rutherford backscattering spectra of the IGZO indicating the signatures of the elements in the device stack, the composition derived from the depth profile is presented in the inset. d) Absorbance spectra of IGZO showing good absorbance in the UV and blue wavelength regime. e) Scanning transmission electron microscope (STEM) image showing distinct layers of the device stack (IGZO~10 nm/SiO_2~180 nm/n-Si). Energy dispersive X-ray (EDX) spectroscopy analysis for element mapping, f) overview image of cross-section used for mapping, g) merged image of individual elements showing distinguishable atomic profile, h)individual atomic profile of indium, gallium, zinc, and oxygen in the device stack.

State of the art gas sensing systems are expensive, power-hungry, and bulky, impeding their large scale deployment for air quality monitoring stations. We successfully demonstrated an integrated thin film electronic microsystem using only two TFTs. This microsystem yields a 5-bit digital output corresponding to the NO_2 concentration without any additional hardware for readout/amplifying and analog to digital conversion (ADC). In the following, we present our results with a discussion of the performance of the IGZO TFT as a gas sensor followed by a demonstration of a TFT based novel integrated microsystem.

Experimental Section

IGZO TFT fabrication process. IGZO thin film (~10 nm) was deposited by RF sputtering using an IGZO ceramic target (In_2O_3-Ga_2O_3-ZnO 1:1:2 mol%) on the gate dielectric (SiO_2). Rapid thermal processing (RTP) was done at 500 ºC for 4 minutes in the oxygen ambiance to improve the TFT device stability. Titanium (Ti) / gold (Au) was deposited using the lift-off process to pattern interdigitated electrodes for a source and drain that yielded width (W) = 583640 µm and L=10 µm.

Passivation of IGZO TFT. Passivation of TFTs was done using chemical vapor deposition of Parylene-C (~1.2 µm thick) in the three-chamber system. In the first chamber, the precursor (2.5 g) was heated at 175 °C under vacuum to generate dimeric vapors. Dimeric vapors were cleaved to monomer gas in the second chamber at an elevated temperature of 650 °C. In the third chamber, the monomer gas was deposited and self-assembled to form the Parylene-C on top of the Si/SiO_2/IGZO substrate at 10E-6 mBar vacuum level. The CVD deposition of parylene-c is the best choice for the conformal coatings[37], insulation and pinhole-free surface[38]. In this case, the sample doesn't undergo higher temperatures and there is no physical damage to the thin film. Moreover, it allows us to extend to flexible substrates.

Electrical characterization. The total flow rate of the gas (carrier gas + toxic gas) was kept constant at 200 SCCM for all the experiments. Sensing performance was monitored using a Precision Multi-meter (Agilent 6 ½ Digital multimeter 34401A), and semiconductor parameter analyzer (Keithley 4200-SCS). The data acquisition and controlling of gas flows were performed through the Labview interface.

Imaging and characterization. A Zeiss Merlin Field Emission Scanning Electron Microscope (FESEM) operated at 5 kV with a beam current of 110 pA was used to capture the cross-sectional image of the passivated device stack. The sample was coated with a layer of 5 nm of Iridium. UV-Visible absorbance of the IGZO thin film was measured using Thermo Scientific Evolution 600 UV-Visible Spectrophotometer. The absorbance was calculated from the reflectance data measured at a scanning speed of 120 nm/min in the range of 190 nm to 900 nm. X-ray photoelectron spectroscopy (XPS) analysis of various conditions of IGZO devices was conducted using the AMICUS XPS instrument (Kratos Analytical, UK). XPS peaks were fitted using Casa-XPS software. The IGZO samples were exposed to X-rays to study its effect; this was done in the XRD Bruker D_2 Phaser instrument. Samples for study were exposed to x-ray source for 4 minutes. A cross-section of the IGZO sample was prepared by a focused ion beam (FIB) using the Helios (FEI) instrument. Scanning transmission electron microscope imaging was performed using a Themis Z (FEI) equipped with the energy dispersive x-ray (EDX) module. High-resolution Rutherford backscattering spectroscopy (RBS) analyses were conducted using an instrument manufactured by Kobe Steel, Ltd. The

average composition and depth profile were obtained by operating the α -source at 400 keV, and with He+ ions (α particles) with a beam size of about 1 mm. AFM imaging was performed using the Bruker Dimension Icon AFM system. For AFM topography imaging, scan rate, integral gain, amplitude set point, and drive frequency were optimized at 0.996 Hz, 2.686, 5.000, 803.8 pm, and 61.29249 kHz, respectively. In addition, lift scan height, input gain, and drive amplitude were set at 108 nm, 5.0, and 500 mV, respectively, to record the surface potential images of IGZO thin film.

Results and discussion

We fabricated a bottom gate top contact IGZO TFT based gas sensor in which IGZO serves the dual role of a channel layer and a sensing layer to detect NO_2. The schematic of the device is as provided in Figure 1a. We followed a bottom to top approach in fabricating the IGZO TFT, as shown in Figure S1 and described in the supplementary information-1 (SI-1). The IGZO thin film is very smooth, with a mean roughness of 0.23 nm, as shown in the atomic force microscopy (AFM) image (Figure 1b). The individual composition of the device stack was analyzed using high-resolution Rutherford backscattering spectroscopy (RBS), as depicted in Figure 1c. As can be seen in Figure 1d, the device showed good absorbance in the UV and blue wavelength regime. The layers of the device stack were distinct, which can be observed in the scanning transmission electron microscope (STEM) image (Figure 1e). Element mapping was performed using energy dispersive X-ray (EDX) spectroscopy, which indicated elements of IGZO within the top ~10 nm, and its interface was distinguishable from SiO_2, as shown in Figure 1f and Figure 1g. The atomic profile of the individual elements (In, Ga, Zn, O, and Si) of the device in the top interface is mapped in Figure 1h.

IGZO TFTs were characterized using a semiconductor parameter analyzer. The devices showed an ON/OFF ratio of ~ 10^7, high linear mobility (7.58 $cm^2V^{-1}s^{-1}$), low subthreshold swing (0.49 $Vdec^{-1}$), and stable electrical characteristics for use as TFT based sensors. Transfer and output characteristics of fabricated devices are as presented in Figure 2a and Figure 2b, respectively. The reported IGZO TFTs possess instabilities because of the traps within the channel layer resulting in shifting the threshold voltage (V_{th}).[39] However, these instabilities could be minimized through fabrication process strategies.[40-41] We optimized the TFT devices to have minimal instabilities through the RTP process; Figure 2c and Figure 2d. show their stability.

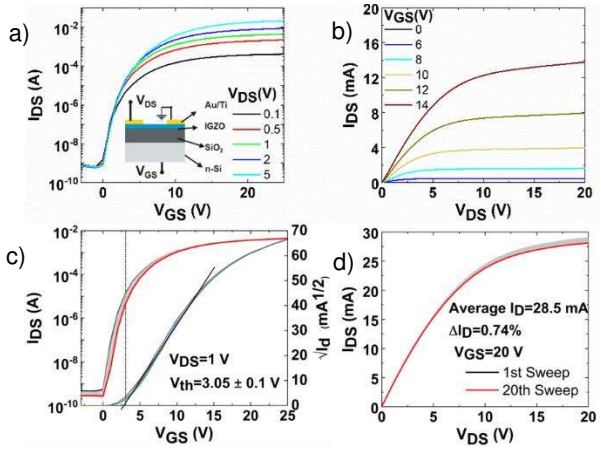

Figure 2a) Transfer and b) output characteristics of the IGZO TFT at various bias voltages. c) Repeatable transfer and d) repeatable output characteristics at constant bias showing the stability of the device at room temperature.

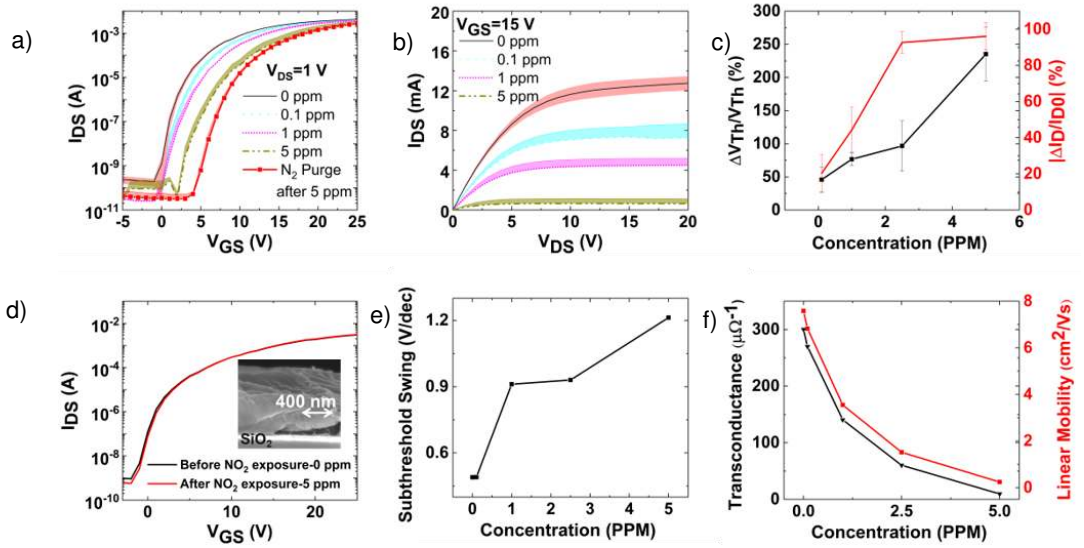

Figure 3a) Transfer and b) Output Characteristics of IGZO TFT sensors after 3 min exposure of 100 ppb to 5 ppm concentrations of NO_2. c) The variation in the V_{th} and the I_D of IGZO TFT for various concentrations of NO_2. d) Transfer characteristics are showing the non-reactive behavior of the IGZO TFT towards NO_2 after passivation with Parylene-C. Variation in other parameters of non-passivated IGZO TFT device in response to the NO_2 concentrations e) subthreshold swing, f) transconductance, and linear field-effect mobility.

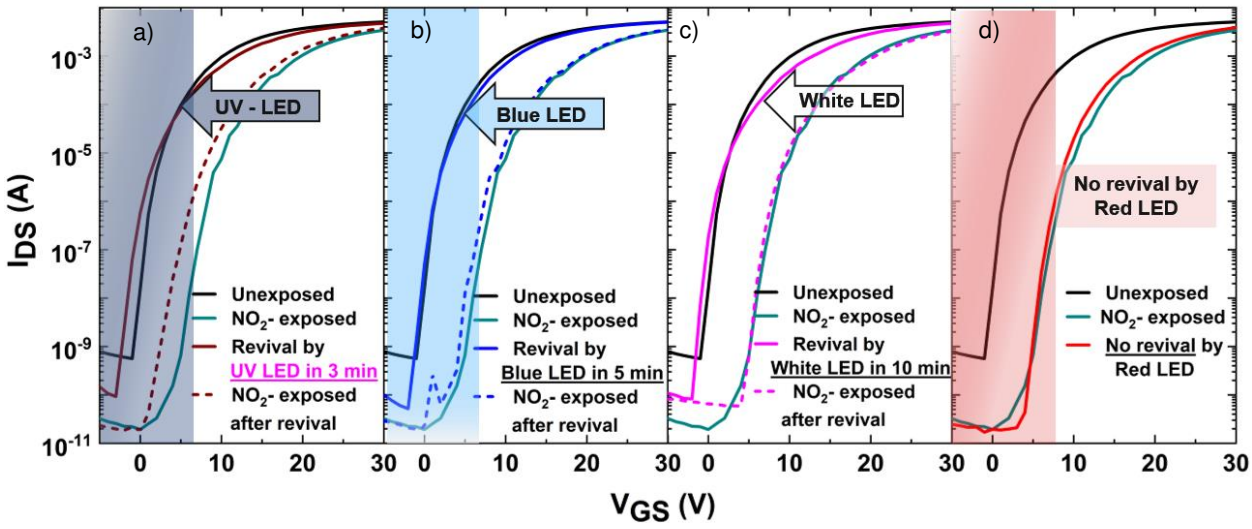

Figure 4. Shows revival of NO_2 exposed IGZO TFT transfer characteristics under illumination of various commercial LEDs of different wavelengths with same intensity a) revival by UV LED (400 nm) in 3 min, b) revival by Blue LED in 5 min (~450 nm), c) revival by White LED in 10 min, d) not revived by Red LED (>635 nm) even after 15 minutes.

Investigation of IGZO TFTs for the gas response. Multiple IGZO TFTs were further tested for their gas response with various toxic gases in the tailor-made gas setup[42] shown in Figure S2. Their concentrations were controlled by diluting them with nitrogen (N_2) as the carrier gas using mass flow controllers. We found that the semiconducting properties of IGZO thin film are susceptible to the NO_2 adsorption at room temperature presented in Figure 3. We monitored the transfer and output characteristics of IGZO TFTs for every minute after exposing the devices to various concentrations (100 ppb to 5 ppm) of NO_2 at room temperature. Transfer characteristics and output characteristics were measured by keeping V_{DS}= 1 V and V_{GS}= 15 V, respectively. It was observed that with the increase in NO_2 concentration, there was a positive shift in the V_{th} and a decrease in the drain current (I_D) of TFT; this is consistent with the reported IGZO TFT based sensors[34, 36] as shown in Figure 3a and Figure 3b. There was a substantial change in the V_{th} and I_D of IGZO TFTs proportional to the concentration of NO_2. We passivated the IGZO TFT using a chemical vapor deposition of Parylene-C. Interestingly, there was no effect of NO_2 on the device characteristics after its exposure to passivated IGZO TFT, as depicted in Figure 3d. This served to make the TFT insensitive to the ambiance which can be used as conventional n-type TFT. Non-passivated IGZO TFT sensor parameters, such as linear field-effect mobility, subthreshold swing, and transconductance in the presence of NO_2, were extracted[31] from transfer characteristics(discussed in SI-2). It was observed that with the increase in NO_2 concentration, subthreshold swing (which describes the steepness of I_D transition from the OFF state to the ON state) increased, as can be seen in Figure 3e. Transconductance and linear field-effect mobility (which determines the conductivity and electronic transport of carriers in the channel) were proportionally reduced with rising NO_2 concentration (as in Figure 3f). The variation in these parameters indicates that there was adequate depletion of charge carriers from the IGZO channel surface due to the interaction with the NO_2 gas, as described in Equation 1. NO_2 is a strong oxidizing agent, where surface carriers of the IGZO channel are involved in the reduction of the NO_2 gas molecules.[43-44]

$$NO_2\,(\text{gas}) + e^-\,(\text{IGZO surface}) \rightarrow NO_2^-\,(\text{ads}) \qquad (1)$$

$$\frac{\Delta V_{th}}{V_{th}}\% = \frac{(V_{th\ \text{after exposure}} - V_{th\ \text{before exposure}})}{V_{th\ \text{before exposure}}} * 100 \qquad (2)$$

$$\frac{\Delta I_D}{I_D}\% = \frac{(I_{D\ \text{after exposure}} - I_{D\ \text{before exposure}})}{I_{D\ \text{before exposure}}} * 100 \qquad (3)$$

From the transfer and output characteristics of the IGZO TFT, the response (%) in terms of V_{th} and I_D was measured using Equation 2 and 3, and as shown in Figure 3c. The V_{th} was extracted from the linear extrapolation of the $\sqrt{I_{DS}}$-V_{GS} curve. In gas or chemical sensors, the recovery of the device is crucial. Since the channel of the TFT was oxidized after NO_2 exposure, these devices could not be recovered even after a prolonged N_2 purge (Figure 3a) owing to the strong bonding of gas molecules with the active area. Similarly, Kim et al. observed the adsorption of NO_2 with an IGZO active layer and could not recover the device after exposure at room temperature. [34, 36] The semiconducting channel properties could be revived only after the application of some external energy. Hence, we explored the revival of TFT sensors using light activation, as IGZO is reported to have excellent photoelectric characteristics.[45] We evaluated the IGZO TFT sensors' revival performance after exposure to 5 ppm of NO_2 by illuminating them with various commercial light-emitting diodes (LEDs) such as UV LED (400 nm), Blue LED (~ 450 nm), White LED and Red LED (~635 nm) of the same intensity (~1 mW/cm^2) mounted at ~2 cm above the active area (Figure S2). We found that gas exposed devices were completely regenerated only under the illumination of UV, Blue, and White LEDs, but not under Red LEDs. It is also evident from the absorbance spectra (Figure 1d) that the absorbance of the devices in the UV and Blue wavelength regimes, and it was close to zero in the Red regime. Revived devices responded to NO_2 gas as pristine devices; the corresponding response and revival times are shown in Figure 4. We also noticed that the recovery time with UV LED (3 min) was much shorter than with Blue (5 min) and White LED (10 min) in the presence of the N_2 purge. However, UV LEDs are harmful to human health and more expensive than Blue LEDs;[46] hence, the rest of the experiments were conducted with the Blue LED alone. The light-activated recovery time without the N_2 purge was longer than in the presence of the N_2 purge during the revival, as shown in Figure S3.

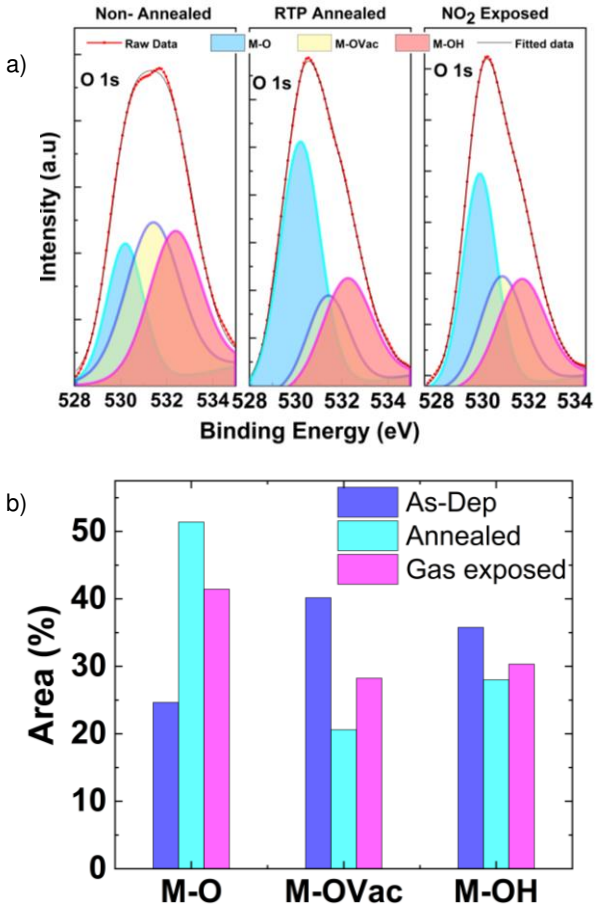

Figure 5a) Deconvoluted X-ray photoelectron Spectroscopy (XPS) of O_{1s} Peaks, b)) composition (area under the peak) of deconvoluted O_{1s} peaks comparing different conditions such as (As-Dep) IGZO, RTP annealed IGZO, gas exposed on RTP Annealed IGZO thin films

Sensing and revival mechanism. A study on the individual role of Indium (In), Gallium (Ga), and Zinc (Zn) in IGZO TFTs revealed that the composition of these elements is critical in determining the electrical properties of the TFTs due to the electronic band structures in the IGZO composite.[47] Indium concentration determines the conductivity of the channel, Ga concentration determines the OFF current that can be tuned to control the ON/OFF ratio, and Zn concentration determines the subthreshold swing of the TFT.[48] The concentration of In in the IGZO is crucial for the sensitivity of NO_2 at room temperature. A previous study[44] showed that In concentration in the composite of IGZO determined the NO_2 adsorption at low temperatures. The higher the In concentration, the higher the sensitivity to NO_2 in the chemi-resistive based sensor at <150 ^oC. We conducted a high-resolution RBS analysis of the IGZO thin film for the precise determination of the depth profile of the active IGZO, as shown in Figure S4a. This analysis indicated that the higher concentrations of In in the thin film led to an increase in carrier density, which made IGZO TFT sensors sensitive to NO_2. Moreover, it was also evident from the EDX analysis that In atomic concentration was relatively higher at the surface of the IGZO layer, as can be seen in Figure S4c. Hence, we posit that a higher In concentration at the surface of the IGZO also favors adsorption of NO_2.

X-ray photoelectron spectroscopy (XPS) was performed on IGZO thin film to understand the effects of NO_2 adsorption; the results are depicted in Figure 5. Three conditions of vacuum processed IGZO thin film were used for the XPS studies: a) as-deposited IGZO sputtered film, b) RTP annealed IGZO thin film (active layer used to fabricate NO_2 Sensor) and the c) NO_2 exposed on RTP annealed IGZO thin film. Figure 5a compares the de-convoluted O_{1s} peaks of these conditions, which correspond to the oxygen in the lattice (M-O), oxygen deficiencies (M-O_{Vac}), and weakly bonded hydroxyl groups (M-OH) centered at the binding energy of 530.3±0.1 eV, 531.3±0.1 eV, 532.3±0.1 eV, respectively. The previous studies[49-50] have shown that these components reflect the electrical behavior of IGZO TFTs in terms of the shift in V_{th}, ON/OFF current, and field-effect mobility. The M-O peak corresponds to the conducting pathways in the channel and improved mobility of the charge carriers, whereas the M-O_{Vac} peak and M-OH correspond to the carrier concentration, defects, and trap sites in the film. Figure 5b compares the areas under O_{1s} peaks of these conditions**.** The improvement in M-O% and reduction in M-O_{Vac} and M-OH% after RTP annealing as compared to the non-annealed device signifies a decrease in the number of trap sites and improved carrier density. This reflects a better performance in terms of stability and ON current, which is in line with the literature.[50-51] To study the effect of NO_2 adsorption, we performed an XPS analysis on an RTP annealed device after prolonged exposure to NO_2 gas. The O_{1s} peak after gas exposure shows a decrease in M-O% and a slight increase in both M-O_{Vac}% and M-OH%. Variations in O_{1s} peaks indicate an increase in trap sites and scattering centers within a few nm of the IGZO thin film, affecting the charge carriers and their mobility. Observed electrical behavior after NO_2 exposure, such as the reduced ON current, decreasing mobility, and positive shift in V_{th}, corroborate the increase in surface defects. Furthermore, the X-ray exposure effect was studied on pristine and NO_2 exposed IGZO TFTs. This study revealed X-rays did not have an effect on the unexposed device (Figure S5a) and did not revive the device after exposure, as shown in Figure S5b. Hence, the observations obtained through XPS analysis on NO_2 exposed samples hold well. From XPS analysis, we conclude that NO_2 was adsorbed on the surface of IGZO, as depicted in the schematic of the sensing mechanism (Figure 6a). The XPS analysis and electrical characteristic**s** indicate that adsorbed NO_2 molecules depleted the charge carriers from the channel, as shown in Figure 6b.

$$NO_2^-(ads) + h^+(\text{Photo generated} - h\upsilon) \rightarrow NO_2(gas) \quad (4)$$

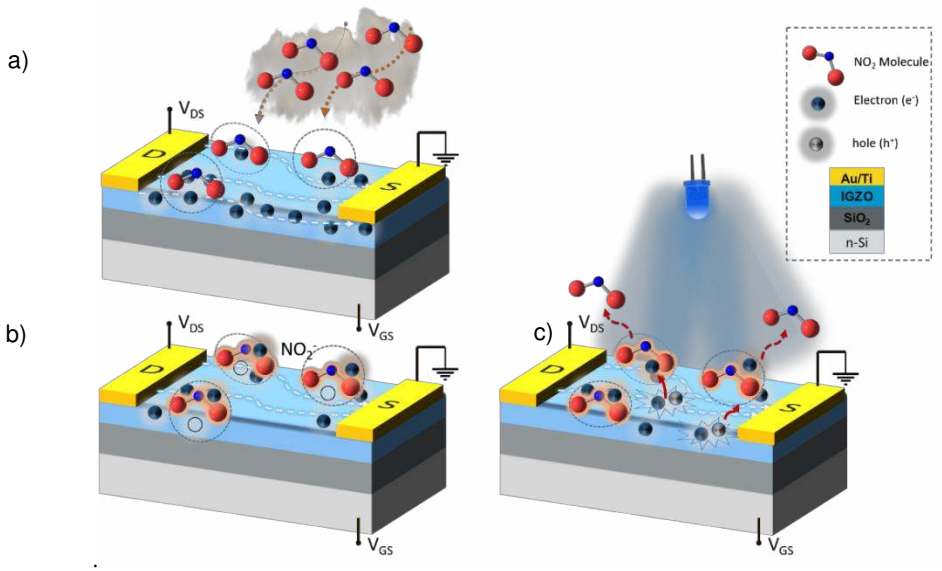

Figure 6. Schematic depiction of sensing and revival mechanisms at a glance a) adsorption of NO_2 molecules on the active layer b) depletion of Surface charge carriers of IGZO c) revival mechanism of the device under LED illumination.

In polycrystalline materials or materials with the higher effective area, gas molecules diffuse through the grain boundaries where higher temperatures are required for active sensing and revival.[52] IGZO thin film is smooth with a mean roughness of 0.23 nm, and it is an amorphous semiconductor without grain boundaries. Hence, there is a minimum probability of gas molecule diffusions. Restricting gas molecules on the IGZO surface requires minimal energy to desorb them, so achieving the revival with LEDs is feasible. Observations of revival after NO_2 exposure with LEDs suggest that photo-carrier generation plays a massive role in regenerating the device by desorbing the ionized molecules (NO_2^-). The holes generated in the IGZO upon illumination neutralize the ionized molecules (NO_2^-) and desorb them from the surface, as described in Equation 4. The presence of N_2 during the revival helps in sweeping away the desorbed molecules making the recovery time short (Figure S3). This desorption mechanism is depicted in Figure 6c. It is consistent with the reported desorbing of O^{2-} molecules on n-type metal oxides,[53-54], and light-activated metal oxide gas sensors.[29] Thus, Figure 6 explains the complete sensing and revival mechanism.

Performance of an IGZO TFT sensor. The response of IGZO TFT as a sensor was further evaluated in the common source (CS) configuration, as shown in Figure 7a. The TFT was operated with V_{DD}=10 V and V_{GS}= 15 V. In this configuration, the effect on the change in I_D was more significant after exposure to NO_2 and measured in terms of voltage across the resistor ($V_R = V_{DD} - I_D * R_D$; $\Delta V_R = -\Delta I_D * R_D$). In this mode, the transient response of TFT was acquired for various concentrations of NO_2 (from 100 ppb to 5 ppm), as shown in Figure 7b. TFT devices were exposed to NO_2 for 3 minutes. Then, after reaching the saturated response, they were revived by being illuminated with blue light (represented as the blue shaded region). The recovery time by illumination was proportional to the exposure concentration of NO_2 gas: the higher the concentration of exposure, the extent of electron-hole pair generation required to recover depleted channel is high and vice versa. A reproducibility study (Figure 7c) was conducted for 5 ppm of NO_2 in the CS configuration. The biasing was optimized in a way that sensor yielded linearity and better sensitivity in the whole concentration region irrespective of the device operation region. The repeatability in response showed that the device was completely recovered by the blue LED, and the response was reproducible at room temperature. The response of devices revived with high temperature has been shown to decrease after a few cycles in IGZO TFT sensors[34] due to partial recovery. In contrast, in our case, the device response was stable for multiple cycles with the LED enabled revival strategy. We also tested the same device after 40 days by keeping it in the air; as can be observed from Figure 7c (in-set), the response was the same as that of an unexposed device, indicating the stability of the device in the air. The responsivity for the 0.1 ppm and 5 ppm concentration exposure of NO_2 for 3 minutes was 37% and 1330%, respectively (Figure 7d).

The fabricated IGZO sensors' sensitivity is better than that of previously reported TFT based NO_2 sensors, as shown in the summary table (Table 1). Reported SMO devices require high temperature (>1000 °C) or complete UV activation for sensing and revival, whereas our device needs visible light activation only during the revival. We also evaluated the IGZO TFTs' response to various harmful oxidizing and reducing gases. The response to 1 ppm NO_2 was higher than to 100 ppm of other gases, such as sulphur dioxide (SO_2), ammonia (NH_3), hydrogen (H_2), methane (CH_4), carbon monoxide (CO), and carbon dioxide (CO_2). The magnitude of the responsivity in V_{th} and I_D from transfer and output characteristics shows high selectivity of IGZO TFT toward NO_2, as shown in Figure 7e and Figure 7f. NO_2 is a strong oxidizing gas, its high electron affinity[55] leading it to possess strong electrophilic properties[56]. The fabricated IGZO channel is an n-type semiconductor with high electron carrier density in the channel, as observed from its electrical behavior. In addition to this, the higher indium concentration in the IGZO favors NO_2 adsorption[44]. All these factors are constructively favoring the IGZO TFT selective to NO_2 when compared to other oxidizing and reducing gases. To further confirm this, we performed the Kelvin probe force microscopy (KPFM) analysis before and after exposing these gases. An average contact potential difference (CPD) was measured in the area of (500 nm X 500 nm) and it was considered to calculate work function, as described in SI-7. Figure S6a indicates the variation in the work function before and immediately after exposing IGZO thin film to NO_2. The dominant adsorption of NO_2 was further confirmed (Figure S6b), where the change in work function showed maximum for NO_2 when compared to other interferon gases indicating the strong oxidizing nature of NO_2. The KPFM and XPS analysis further validate the Equation 1.

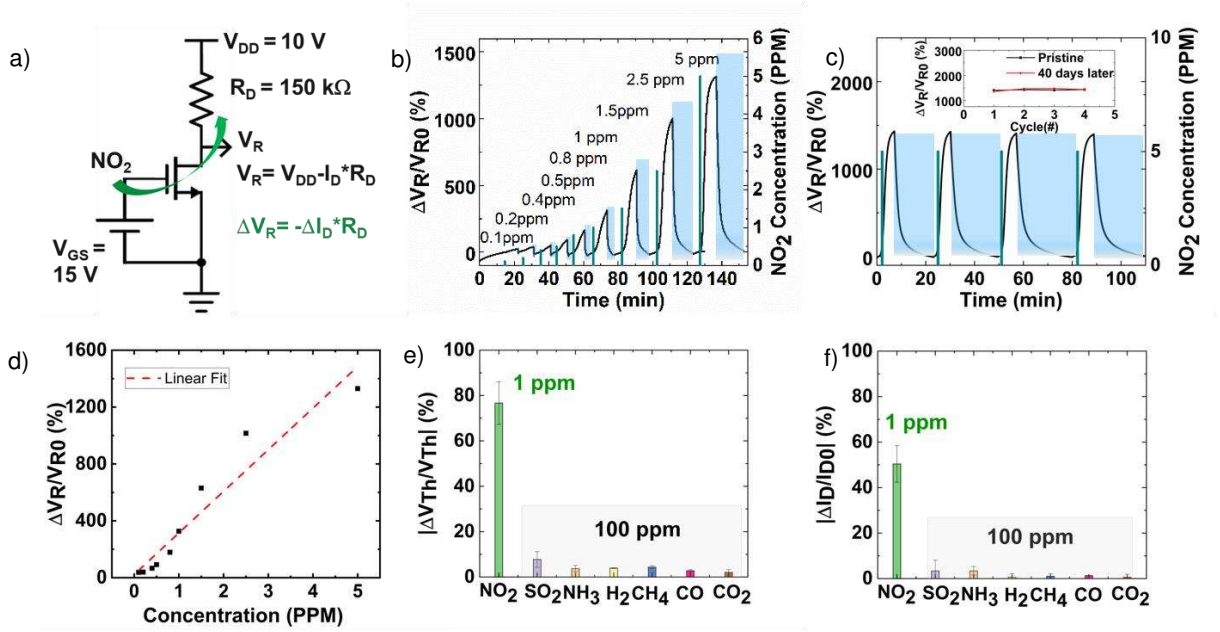

Figure 7a) IGZO TFT implemented in the common source (CS) configuration to assess the change in I_D due to the NO_2 adsorption. b) Transient response of TFT for 3-minute exposure of 100 ppb to 5 ppm NO_2 and recovered by illuminating blue LED as represented in the blue shaded region. c) Reproducible transient response of IGZO TFT at 5 ppm NO_2 concentration for 3 min exposure in the CS Configuration and the reproducible response of device stored in the Air after 40 days after first exposure (the in-set). d) Concentration versus calculated responsivity. Selectivity study results by exposing various harmful gases to IGZO TFT sensors e) variation in the V_{th} f) variation in the I_D.

Table 1. Comparison of the TFT based gas sensors' performance.

TFT Based NO_2 gas sensors					
Active material	LOD (ppm)	Sensing condition	Recovery condition	Responsivity (5ppm) ($\Delta I_D/I_{D0}$ (%))	Refs
IGZO (TFT)	0.5	RT and 100 °C	100 °C	-95.7	[34]
IGZO (TFT)	2	RT(UV)	RT(UV)	-17.35	[35]
MOS_2 (Pt decorated)	0.5	RT	RT	~18	[57]
PCDTBT (OFET)	1	RT	RT	~50	[58]
CuPc (OFET)	0.5	RT	RT	~10	[59]
		RT (UV)	RT	500	
IGZO (TFT)	**0.1**	**RT**	**RT (Vis)**	**-99.8**	**This work**

IGZO thin film electronics-based sensor microsystem for toxic gas detection. After our detailed investigation of the IGZO TFT as a NO_2 sensor by studying its electrical behavior and response in various circuit configurations. Non-passivated and passivated TFTs allowed us to design an integrated smart sensor system incorporating readout circuits and an analog to digital converter that could be directly integrated with the Internet of Things (IoT) sensory nodes.

We devised a sensor microsystem to detect the presence of NO_2 and quantify its concentration digitally; the 3D schematic depicting integrated IGZO TFT sensor and passivated TFT is provided in Figure 8a. Its fabrication process flow is briefly detailed in the SI-8. In this design, the IGZO TFT sensor in the diode configuration is cascoded with the passivated TFT is shown in Figure 8b. The TFT sensor is biased with constant VDD, and the gate of passivated TFT (n-type) is connected to the variable voltage source. The IGZO TFT sensor at a constant bias controls the current in the branch based on the ambient conditions. The gate-source voltage (V_{GS}) of passivated TFT can be controlled to maintain different levels of current in the branch, thereby tuning the voltage at the input of the inverter (V_{inv}) node. The inverter output (V_{Bit}) makes the transition to logic "high" when V_{inv} decreases beyond the voltage level of input logic "low" of the inverter (1.8 V). The change in NO_2 concentration induces a change in V_{th} and I_D in the TFT sensor, and the V_{inv} changes correspondingly when the system is exposed to NO_2. Likewise, multiple V_{GS} amplitudes are tuned to make V_{inv} reach beyond the threshold (input logic low) of the inverter, which triggers the output (logic high) for various NO_2 concentrations.

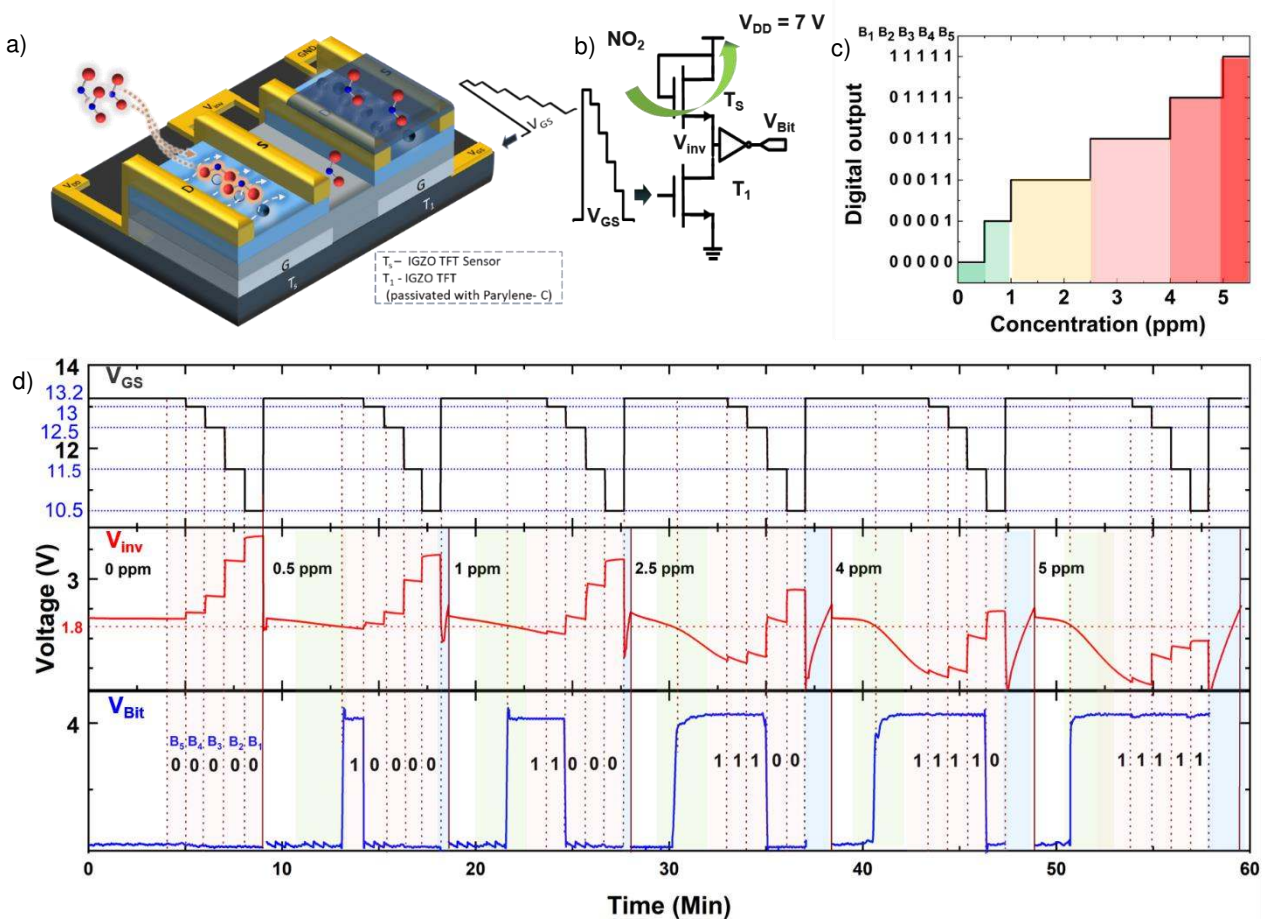

Figure 8a) 3-D schematic of microsystem showing the IGZO TFT as the sensor in diode configuration cascoded with IGZO passivated TFT (passivated with the Parylene-C), b) Circuit schematic of 5-bit digital gas-sensitive thin film electronic-based microsystem, voltage at the gate (V_{GS}) is to be varied sequentially to obtain digital output corresponding to Gas concentration. (V_{DD}= 7 V) c) The output of the 5-bit microsystem indicating the digital thermometer code corresponding to the NO_2 concentration higher than 0.5 ppm, 1 ppm, 2.5 ppm, 4 ppm, and 5 ppm. d) Shows applied V_{GS}, voltage at input of inverter node (V_{inv}), corresponding digital output (V_{Bit}) in the transient analysis of integrated microsystem when exposed to various concentrations of NO_2 and colors indicate the duration of sequential operations (Green shade indicates the exposure of the gas, pink shade indicates the sequential V_{GS} voltage (high to low) applied to read the concentration and blue shade indicates the revival of the TFT sensor).

This system can be operated in two modes: a) to detect the presence of NO_2 at a calibrated concentration that yields output "1" in the presence of NO_2 and vice-versa; and b) to detect and digitally quantify NO_2 concentration. In the first mode, by applying constant V_{GS} voltage, and the system can be tuned to detect the particular concentration of NO_2 (calibrated concentration). In the second mode, the system has to be operated sequentially to obtain the digital output. Five V_{GS} levels are tuned to quantify five different concentrations that yield a 5-bit digital thermometer code. Out of these V_{GS} voltages, passivated TFT is biased at a higher V_{GS} voltage. When there is NO_2 exposure, the inverter triggers a transition after a specific concentration. Subsequently, V_{GS} voltages (tuned voltages) are applied in steps from high to low to quantify the concentration of gas, and the corresponding digital output can be read.

A transient analysis was conducted by exposing the system to NO_2 concentrations ranging from 0.5 ppm to 5 ppm. Figure 8d shows the V_{inv} and the corresponding digital output (V_{Bit}) in the transient analysis of the integrated microsystem. When the system was not exposed to NO_2, the digital output of the system was "0" at every tuned V_{GS} voltage, since the V_{inv} did not cross beyond the inverter logic low threshold (1.8 V). In contrast, when the system was exposed to more than 0.5 ppm, the inverter output was high ("1") within a minute after exposure, and sequential V_{GS} pulses were applied to read the corresponding concentration. The digital output of the system quantifying the NO_2 concentration is shown in Figure 8c. The TFT sensor was revived using light illumination until the system reset (output "0") after reading the concentration of the gas. The applied V_{GS} pulse width to read the concentration of ambient gas can also be in the order of a few seconds, but for demonstration purposes, we used a one-minute width for each level. In this configuration, we needed only one TFT sensor and one passivated TFT. The resolution of the output can be extended by adjusting the n-levels of V_{GS} to yield n- bit digital output. Since the number of bits is fully programmable by adjusting the V_{GS} voltage levels, it has the potential to detect a wide range of concentrations and provide a digital output. This kind of system can be easily integrated into various gas sensing platforms. Thus, we demonstrated a digital thin film electronic-based microsystem without any need for readout circuits and additional analog to digital converters, which paves for power-efficient and inexpensive gas sensing systems.

Conclusion

We demonstrated an integrated sensory microsystem, with output in a digital 5-bit thermometer code format proportional to the NO_2 concentration. The devised microsystem is a standalone sensing unit and the first of its kind. It is inexpensive, compact, and easily deployable at a large scale for air quality monitoring stations.

The crucial component of the microsystem is an indigenously developed IGZO based TFT gas sensor for low concentration NO_2 detection. This is the first report of a metal oxide TFT based gas sensor for room temperature sensing and to regenerate the device with light activation. The IGZO thin film is used as both an active layer for sensing and a channel layer for the fabricated IGZO TFT sensor. The surface of the active IGZO layer is oxidized at room temperature due to the adsorption of NO_2, thereby significantly increasing the resistance of the channel and resulting in a shift of the threshold voltage and drain current. Thus, the IGZO sensor shows an excellent sensitivity of 12 nA/ppb and 15 mV/ppb for I_D and V_{th}, respectively. Furthermore, we reported its selectivity performance by comparing different oxidizing and reducing gases. We successfully built a 5-bit gas concentration to digital converter (GCDC) incorporating readout and ADC modules with IGZO TFT as a fundamental element. We measured the sensor's limit of detection to be as low as 100 ppb. The developed microsystem has the potential to be integrated with the Internet of Things (IoT) nodes for smart cities.

ASSOCIATED CONTENT

Supporting information

Supporting Information Available: The following file is available free of charge.

Supporting information file indicates the process flow of the IGZO TFT sensor; TFT device parameter extraction and calculations; test setup; Effect of nitrogen purge during revival; the depth profile indicating atomic densities; effect of the x-ray on a device; process steps of the microsystem.

AUTHOR INFORMATION

Corresponding Author

E-mail: khaled.salama@kaust.edu.sa.

Author Contributions

V. Mani Teja, Sandeep G. Surya contributed equally.

Funding Sources

The research reported in this manuscript was supported by the funding of King Abdullah University of Science and technology.

ACKNOWLEDGMENT

We are thankful for Prof. TH Hou and Yi-Hsui Lai from National Chiao-Tung University, Taiwan (NCTU, Taiwan), for valuable discussions. We are also thankful to thin film (TF) lab, Nano-fabrication (NCL), and imaging and characterization (IAC) core-labs' staff of KAUST for their help throughout.

REFERENCES

(1) Caplin, A.; Ghandehari, M.; Lim, C.; Glimcher, P.; Thurston, G. Advancing environmental exposure assessment science to benefit society. Nature Communications **2019,** *10* (1), 1236, DOI: 10.1038/s41467-019-09155-4.

(2) Anenberg, S. C.; Miller, J.; Minjares, R.; Du, L.; Henze, D. K.; Lacey, F.; Malley, C. S.; Emberson, L.; Franco, V.; Klimont, Z.; Heyes, C. Impacts and mitigation of excess diesel-related NOx emissions in 11 major vehicle markets. *Nature* **2017,** *545*, 467, DOI: 10.1038/nature22086

https://www.nature.com/articles/nature22086#supplementary-information.

(3) Loghin, F. C.; Falco, A.; Albrecht, A.; Salmerón, J. F.; Becherer, M.; Lugli, P.; Rivandeneyra, A. A Handwriting Method for Low-Cost Gas Sensors. *ACS Applied Materials and Interfaces* **2018,** *10* (40), 34683-34689, DOI: 10.1021/acsami.8b08050.

(4) Spinelle, L.; Gerboles, M.; Villani, M. G.; Aleixandre, M.; Bonavitacola, F. Field calibration of a cluster of low-cost commercially available sensors for air quality monitoring. Part B: NO, CO and CO_2. *Sensors and Actuators B: Chemical* **2017,** *238*, 706-715, DOI: https://doi.org/10.1016/j.snb.2016.07.036.

(5) Tchalala, M. R.; Bhatt, P. M.; Chappanda, K. N.; Tavares, S. R.; Adil, K.; Belmabkhout, Y.; Shkurenko, A.; Cadiau, A.; Heymans, N.; De Weireld, G.; Maurin, G.; Salama, K. N.; Eddaoudi, M. Fluorinated MOF platform for selective removal and sensing of SO_2 from flue gas and air. *Nat Commun* **2019,** *10* (1), 1328, DOI: 10.1038/s41467-019-09157-2.

(6) Lin, Y.; Chen, J.; Tavakoli, M. M.; Gao, Y.; Zhu, Y.; Zhang, D.; Kam, M.; He, Z.; Fan, Z. Printable Fabrication of a Fully Integrated and Self-Powered Sensor System on Plastic Substrates. *Advanced Materials* **2019,** *31* (5), DOI: 10.1002/adma.201804285.

(7) Pham, T.; Li, G.; Bekyarova, E.; Itkis, M. E.; Mulchandani, A. MoS_2 -Based Optoelectronic Gas Sensor with Sub-parts-per-billion Limit of NO_2 Gas Detection. *ACS Nano* **2019,** *13* (3), 3196-3205, DOI: 10.1021/acsnano.8b08778.

(8) Chernikova, V.; Yassine, O.; Shekhah, O.; Eddaoudi, M.; Salama, Khaled N. Highly sensitive and selective SO_2 MOF sensor: the integration of MFM-300 MOF as a sensitive layer on a capacitive interdigitated electrode. *Journal of Materials Chemistry A* **2018,** *6* (14), 5550-5554, DOI: 10.1039/c7ta10538j.

(9) Yuan, H.; Aljneibi, S. A. A. A.; Yuan, J.; Wang, Y.; Liu, H.; Fang, J.; Tang, C.; Yan, X.; Cai, H.; Gu, Y.; Pennycook, S. J.; Tao, J.; Zhao, D. ZnO Nanosheets Abundant in Oxygen Vacancies Derived from Metal-Organic Frameworks for ppb-Level Gas Sensing. *Advanced Materials* **2019,** *31* (11), DOI: 10.1002/adma.201807161.

(10)https://www.osha.gov/dts/sltc/methods/inorganic/id182/id182.pdf.

(11) Kim, K. H.; Jahan, S. A.; Kabir, E. A review on human health perspective of air pollution with respect to allergies and asthma. *Environment International* **2013,** *59*, 41-52, DOI: 10.1016/j.envint.2013.05.007.

(12) Andersen, Z. J.; Bønnelykke, K.; Hvidberg, M.; Jensen, S. S.; Ketzel, M.; Loft, S.; Sørensen, M.; Tjønneland, A.; Overvad, K.; Raaschou-Nielsen, O. Long-term exposure to air pollution and asthma hospitalisations in older adults: A cohort study. *Thorax* **2012,** *67* (1), 6-11, DOI: 10.1136/thoraxjnl-2011-200711.

(13) Tawfik, S. M.; Sharipov, M.; Kakhkhorov, S.; Elmasry, M. R.; Lee, Y. I. Multiple Emitting Amphiphilic Conjugated Polythiophenes-Coated CdTe QDs for Picogram Detection of Trinitrophenol Explosive and Application Using Chitosan Film and Paper-Based Sensor Coupled with Smartphone. *Advanced Science* **2019,** *6* (2), DOI: 10.1002/advs.201801467.

(14) Wang, C.; Yin, L.; Zhang, L.; Xiang, D.; Gao, R. Metal Oxide Gas Sensors: Sensitivity and Influencing Factors. *Sensors* **2010,** *10* (3), DOI: 10.3390/s100302088.

(15) Wang, Z.; Nayak, P. K.; Caraveo-Frescas, J. A.; Alshareef, H. N. Recent Developments in p-Type Oxide Semiconductor Materials and Devices. *Advanced Materials* **2016,** *28* (20), 3831-3892, DOI: 10.1002/adma.201503080.

(16) Bogue, R. Detecting gases with light: A review of optical gas sensor technologies. *Sensor Review* **2015,** *35* (2), 133-140, DOI: 10.1108/SR-09-2014-696.

(17) Petculescu, A.; Hall, B.; Fraenzle, R.; Phillips, S.; Lueptow, R. M. A prototype acoustic gas sensor based on attenuation. *Journal of the Acoustical Society of America* **2006,** *120* (4), 1779-1782, DOI: 10.1121/1.2336758.

(18) Kim, K.-H. Performance characterization of the GC/PFPD for H2S, CH3SH, DMS, and DMDS in air. *Atmospheric Environment* **2005,** *39* (12), 2235-2242, DOI: https://doi.org/10.1016/j.atmosenv.2004.12.039.

(19) Vahidpour, F.; Oberländer, J.; Schöning, M. J. Flexible Calorimetric Gas Sensors for Detection of a Broad Concentration Range of Gaseous Hydrogen Peroxide: A Step Forward to Online Monitoring of Food-Package Sterilization Processes. *physica status solidi (a)* **2018,** *215* (15), DOI: 10.1002/pssa.201800044.

(20) Dey, A. Semiconductor metal oxide gas sensors: A review. *Materials Science and Engineering: B* **2018,** *229*, 206-217, DOI: 10.1016/j.mseb.2017.12.036.

(21) Casals, O.; Markiewicz, N.; Fabrega, C.; Gracia, I.; Cane, C.; Wasisto, H. S.; Waag, A.; Prades, J. D. A Parts Per Billion (ppb) Sensor for NO2 with Microwatt (muW) Power Requirements Based on Micro Light Plates. *ACS Sens* **2019,** *4* (4), 822-826, DOI: 10.1021/acssensors.9b00150.

(22) Haiduk, Y. S.; Khort, A. A.; Lapchuk, N. M.; Savitsky, A. A. Study of WO3–In2O3 nanocomposites for highly sensitive CO and NO2 gas sensors. *Journal of Solid State Chemistry* **2019,** *273*, 25-31, DOI: 10.1016/j.jssc.2019.02.023.

(23) Wang, J.; Yu, M.; Xia, Y.; Li, X.; Yang, C.; Komarneni, S. On-chip grown ZnO nanosheet-array with interconnected nanojunction interfaces for enhanced optoelectronic NO2 gas sensing at room temperature. *J Colloid Interface Sci* **2019,** *554*, 19-28, DOI: 10.1016/j.jcis.2019.06.085.

(24) Assen, A. H.; Yassine, O.; Shekhah, O.; Eddaoudi, M.; Salama, K. N. MOFs for the Sensitive Detection of Ammonia: Deployment of fcu-MOF Thin Films as Effective Chemical Capacitive Sensors. *ACS Sens* **2017,** *2* (9), 1294-1301, DOI: 10.1021/acssensors.7b00304.

(25) Fang, X.; Zong, B.; Mao, S. Metal-Organic Framework-Based Sensors for Environmental Contaminant Sensing. *Nanomicro Lett* **2018,** *10* (4), 64, DOI: 10.1007/s40820-018-0218-0.

(26) Yassine, O.; Shekhah, O.; Assen, A. H.; Belmabkhout, Y.; Salama, K. N.; Eddaoudi, M. H_2S Sensors: Fumarate-Based fcu-MOF Thin Film Grown on a Capacitive Interdigitated Electrode. *Angewandte Chemie - International Edition* **2016,** *55* (51), 15879-15883, DOI: 10.1002/anie.201608780.

(27) Sapsanis, C.; Omran, H.; Chernikova, V.; Shekhah, O.; Belmabkhout, Y.; Buttner, U.; Eddaoudi, M.; Salama, K. N. Insights on Capacitive Interdigitated Electrodes Coated with MOF Thin Films: Humidity and VOCs Sensing as a Case Study. *Sensors (Basel)* **2015,** *15* (8), 18153-66, DOI: 10.3390/s150818153.

(28) Hosseini, Z. S.; zad, A. I.; Mortezaali, A. Room temperature H2S gas sensor based on rather aligned ZnO nanorods with flower-like structures. *Sensors and Actuators B: Chemical* **2015,** *207*, 865-871, DOI: https://doi.org/10.1016/j.snb.2014.10.085.

(29) Xu, F.; Ho, H. P. Light-Activated Metal Oxide Gas Sensors: A Review. *Micromachines (Basel)* **2017,** *8* (11), DOI: 10.3390/mi8110333.

(30) Nomura, K.; Ohta, H.; Takagi, A.; Kamiya, T.; Hirano, M.; Hosono, H. Room-temperature fabrication of transparent flexible thin-film transistors using amorphous oxide semiconductors. *Nature* **2004,** *432* (7016), 488-492, DOI: 10.1038/nature03090.

(31) Petti, L.; Münzenrieder, N.; Vogt, C.; Faber, H.; Büthe, L.; Cantarella, G.; Bottacchi, F.; Anthopoulos, T. D.; Tröster, G. Metal oxide semiconductor thin-film transistors for flexible electronics. *Applied Physics Reviews* **2016,** *3* (2), DOI: 10.1063/1.4953034.

(32) Kang, D.; Lim, H.; Kim, C.; Song, I.; Park, J.; Park, Y.; Chung, J. Amorphous gallium indium zinc oxide thin film transistors: Sensitive to oxygen molecules. *Applied Physics Letters* **2007,** *90* (19), DOI: 10.1063/1.2723543.

(33) Cho, N. G.; Kim, I.-D. NO2 gas sensing properties of amorphous InGaZnO4 submicron-tubes prepared by polymeric fiber templating route. *Sensors and Actuators B: Chemical* **2011,** *160* (1), 499-504, DOI: 10.1016/j.snb.2011.08.017.

(34) Kim, K. S.; Ahn, C. H.; Jung, S. H.; Cho, S. W.; Cho, H. K. Toward Adequate Operation of Amorphous Oxide Thin-Film Transistors for Low-Concentration Gas Detection. *ACS Appl Mater Interfaces* **2018,** *10* (12), 10185-10193, DOI: 10.1021/acsami.7b18657.

(35) Knobelspies, S.; Bierer, B.; Daus, A.; Takabayashi, A.; Salvatore, G. A.; Cantarella, G.; Ortiz Perez, A.; Wollenstein, J.; Palzer, S.; Troster, G. Photo-Induced Room-Temperature Gas Sensing with a-IGZO Based Thin-Film Transistors Fabricated on Flexible Plastic Foil. *Sensors (Basel)* **2018,** *18* (2), DOI: 10.3390/s18020358.

(36) Park, M.-J.; Jeong, H.-S.; Joo, H.-J.; Jeong, H.-Y.; Song, S.-H.; Kwon, H.-I. Improvement of NO2 gas-sensing properties in InGaZnO thin-film transistors by a pre-biasing measurement method. *Semiconductor Science and Technology* **2019,** *34* (6), DOI: 10.1088/1361-6641/ab2155.

(37) Selvarasah, S.; Li, X.; Busnaina, A.; Dokmeci, M. R. Parylene-C passivated carbon nanotube flexible transistors. *Applied Physics Letters* **2010,** *97* (15), 153120, DOI: 10.1063/1.3499758.

(38) Kwon, H. J.; Ye, H.; An, T. K.; Hong, J.; Park, C. E.; Choi, Y.; Shin, S.; Lee, J.; Kim, S. H.; Li, X. Highly stable flexible organic field-effect transistors with Parylene-C gate dielectrics on a flexible substrate. *Organic Electronics* **2019,** *75*, DOI: 10.1016/j.orgel.2019.105391.

(39) Lee, J.-M.; Cho, I.-T.; Lee, J.-H.; Kwon, H.-I. Bias-stress-induced stretched-exponential time dependence of threshold voltage shift in InGaZnO thin film transistors. *Applied Physics Letters* **2008,** *93* (9), DOI: 10.1063/1.2977865.

(40) Nomura, K.; Kamiya, T.; Hirano, M.; Hosono, H. Origins of threshold voltage shifts in room-temperature deposited and annealed a-In-Ga-Zn-O thin-film transistors. *Applied Physics Letters* **2009,** *95* (1), DOI: 10.1063/1.3159831.

(41) Nomura, K.; Kamiya, T.; Ohta, H.; Hirano, M.; Hosono, H. Defect passivation and homogenization of amorphous oxide thin-film transistor by wet O_2 annealing. *Applied Physics Letters* **2008,** *93* (19), DOI: 10.1063/1.3020714.

(42) Chappanda, K. N.; Chaix, A.; Surya, S. G.; Moosa, B. A.; Khashab, N. M.; Salama, K. N. Trianglamine hydrochloride crystals for a highly sensitive and selective humidity sensor. *Sensors and Actuators B: Chemical* **2019,** *294*, 40-47, DOI: 10.1016/j.snb.2019.05.008.

(43) Belysheva, T. V.; Bogovtseva, L. P.; Kazachkov, E. A.; Serebryakova, N. V. Gas-Sensing Properties of Doped In_2O_3 Films as Sensors for NO_2 in Air. *Journal of Analytical Chemistry* **2003,** *58* (6), 583-587, DOI: 10.1023/A:1024176505338.

(44) Vorobyeva, N.; Rumyantseva, M.; Filatova, D.; Spiridonov, F.; Zaytsev, V.; Zaytseva, A.; Gaskov, A. Highly Sensitive ZnO(Ga, In) for Sub-ppm Level NO_2 Detection: Effect of Indium Content. *Chemosensors* **2017,** *5* (2), DOI: 10.3390/chemosensors5020018.

(45) Kang, Y.; Song, H.; Nahm, H. H.; Jeon, S. H.; Cho, Y.; Han, S. Intrinsic nature of visible-light absorption in amorphous semiconducting oxides. *APL Materials* **2014,** *2* (3), DOI: 10.1063/1.4868175.

(46) Zhang, C.; Wang, J.; Olivier, M. G.; Debliquy, M. Room temperature nitrogen dioxide sensors based on N719-

dye sensitized amorphous zinc oxide sensors performed under visible-light illumination. *Sensors and Actuators, B: Chemical* **2015,** *209*, 69-77, DOI: 10.1016/j.snb.2014.11.090.

(47) Iwasaki, T.; Itagaki, N.; Den, T.; Kumomi, H.; Nomura, K.; Kamiya, T.; Hosono, H. Combinatorial approach to thin-film transistors using multicomponent semiconductor channels: An application to amorphous oxide semiconductors in In–Ga–Zn–O system. *Applied Physics Letters* **2007,** *90* (24), DOI: 10.1063/1.2749177.

(48) Kim, D.; Koo, C. Y.; Song, K.; Jeong, Y.; Moon, J. Compositional influence on sol-gel-derived amorphous oxide semiconductor thin film transistors. *Applied Physics Letters* **2009,** *95* (10), DOI: 10.1063/1.3225555.

(49) Chen, C.; Yang, B. R.; Li, G.; Zhou, H.; Huang, B.; Wu, Q.; Zhan, R.; Noh, Y. Y.; Minari, T.; Zhang, S.; Deng, S.; Sirringhaus, H.; Liu, C. Analysis of Ultrahigh Apparent Mobility in Oxide Field-Effect Transistors. *Adv Sci (Weinh)* **2019,** *6* (7), 1801189, DOI: 10.1002/advs.201801189.

(50) Kim, W. G.; Tak, Y. J.; Du Ahn, B.; Jung, T. S.; Chung, K. B.; Kim, H. J. High-pressure Gas Activation for Amorphous Indium-Gallium-Zinc-Oxide Thin-Film Transistors at 100 degrees C. *Sci Rep* **2016,** *6*, 23039, DOI: 10.1038/srep23039.

(51) Lee, K. H.; Park, J. H.; Yoo, Y. B.; Jang, W. S.; Oh, J. Y.; Chae, S. S.; Moon, K. J.; Myoung, J. M.; Baik, H. K. Effects of solution temperature on solution-processed high-performance metal oxide thin-film transistors. *ACS Appl Mater Interfaces* **2013,** *5* (7), 2585-92, DOI: 10.1021/am3032629.

(52) Shen, Y.; Yamazaki, T.; Liu, Z.; Meng, D.; Kikuta, T.; Nakatani, N. Influence of effective surface area on gas sensing properties of WO3 sputtered thin films. *Thin Solid Films* **2009,** *517* (6), 2069-2072, DOI: 10.1016/j.tsf.2008.10.021.

(53) Tian, X.; Yang, X.; Yang, F.; Qi, T. A visible-light activated gas sensor based on perylenediimide-sensitized SnO2 for NO2 detection at room temperature. *Colloids and Surfaces A: Physicochemical and Engineering Aspects* **2019,** *578*, 123621, DOI: https://doi.org/10.1016/j.colsurfa.2019.123621.

(54) Chen, C.-Y.; Retamal, J. R. D.; Wu, I. W.; Lien, D.-H.; Chen, M.-W.; Ding, Y.; Chueh, Y.-L.; Wu, C.-I.; He, J.-H. Probing Surface Band Bending of Surface-Engineered Metal Oxide Nanowires. *ACS Nano* **2012,** *6* (11), 9366-9372, DOI: 10.1021/nn205097e.

(55) Gurlo, A.; Bârsan, N.; Ivanovskaya, M.; Weimar, U.; Göpel, W. In2O3 and MoO3–In2O3 thin film semiconductor sensors: interaction with NO2 and O3. *Sensors and Actuators B: Chemical* **1998,** *47* (1), 92-99, DOI: https://doi.org/10.1016/S0925-4005(98)00033-1.

(56) Bai, S.; Hu, J.; Xu, X.; Luo, R.; Li, D.; Chen, A.; Liu, C. C. Gas sensing properties of quantum-sized ZnO nanoparticles for NO_2 *IEEE Sensors Journal* **2012,** *12* (5), 1234-1238, DOI: 10.1109/JSEN.2011.2167507.

(57) Hong, H. S.; Phuong, N. H.; Huong, N. T.; Nam, N. H.; Hue, N. T. Highly sensitive and low detection limit of resistive NO2 gas sensor based on a MoS2/graphene two-dimensional heterostructures. *Applied Surface Science* **2019,** *492*, 449-454, DOI: 10.1016/j.apsusc.2019.06.230.

(58) Kumar, A.; Jha, P.; Singh, A.; Chauhan, A. K.; Gupta, S. K.; Aswal, D. K.; Muthe, K. P.; Gadkari, S. C. Modeling of gate bias controlled NO 2 response of the PCDTBT based organic field effect transistor. *Chemical Physics Letters* **2018,** *698*, 7-10, DOI: 10.1016/j.cplett.2018.02.043.

(59) Huang, W.; Zhuang, X.; Melkonyan, F. S.; Wang, B.; Zeng, L.; Wang, G.; Han, S.; Bedzyk, M. J.; Yu, J.; Marks, T. J.; Facchetti, A. UV-Ozone Interfacial Modification in Organic Transistors for High-Sensitivity NO2 Detection. *Adv Mater* **2017,** *29* (31), DOI: 10.1002/adma.201701706.

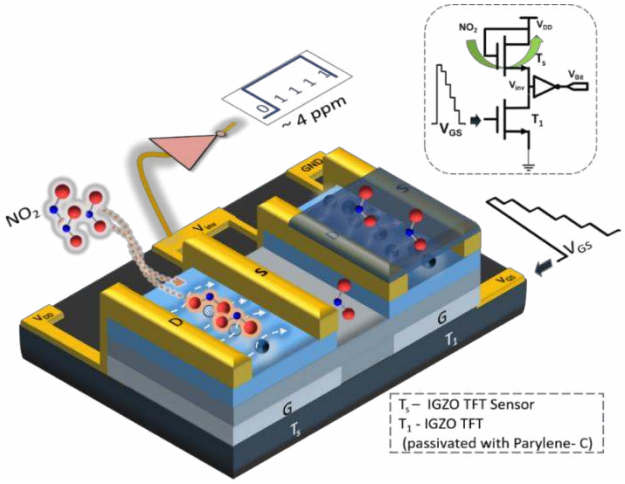

The 3D schematic of the demonstrated microsystem using developed IGZO sensor for detecting NO_2 and its integration with the passivated IGZO TFT as a circuit element. This microsystem yields 5-bit digital output corresponding to the NO_2 concentration.

Table of Contents Artwork